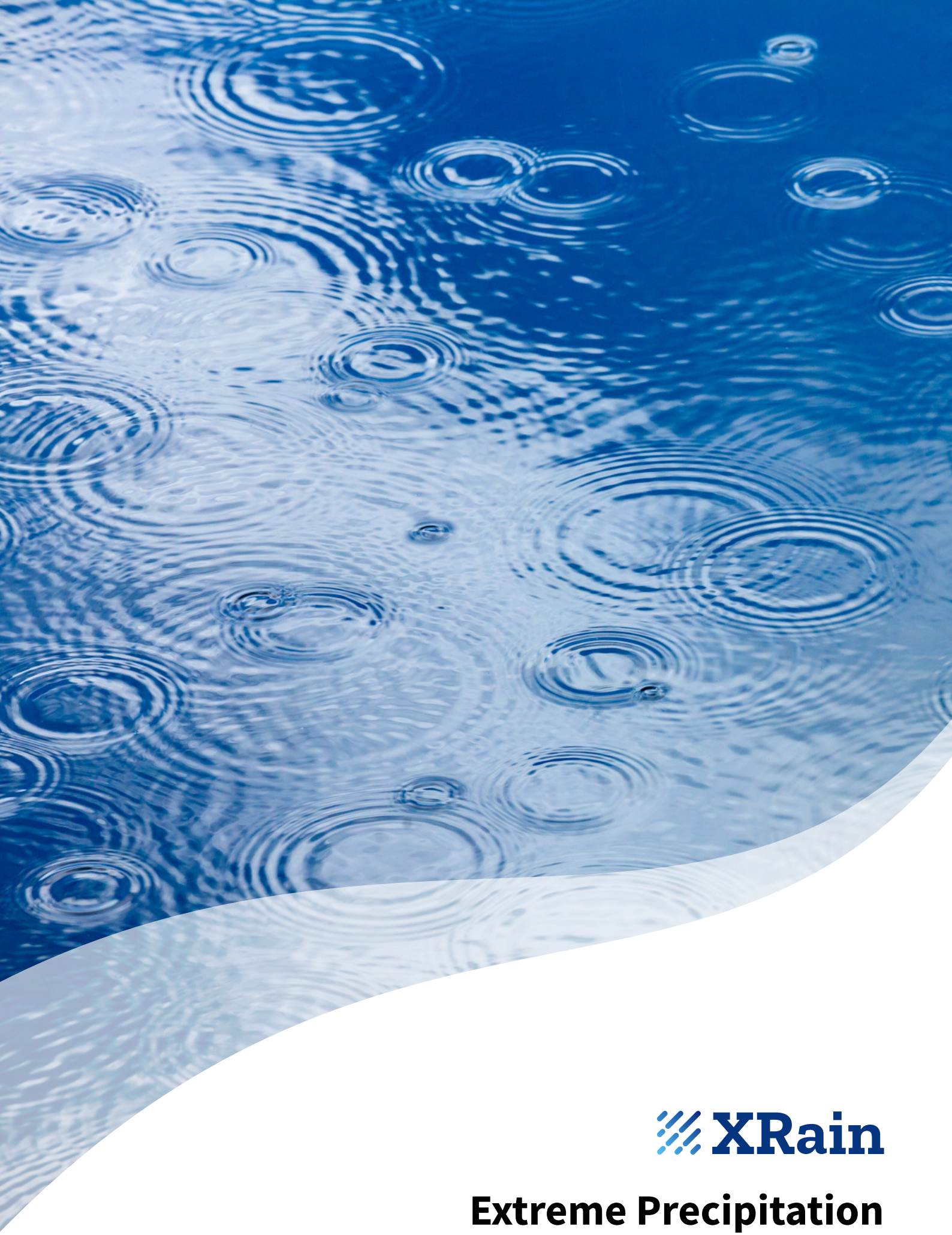

XRain

Extreme Precipitation Statistics on a Global Scale

Executive Summary

Extreme precipitation statistics are used for modelling the flooding that might occur at a location, and are also known as *design rainfall*, *precipitation frequency*, *intensity-duration-frequency* or *depth-duration-frequency*. Traditionally these are derived from long-term rain gauge records. However there are many parts of the world that are physically distant from available rain gauges, making it challenging to estimate extreme statistics. XRain instead derives these statistics from a 20-year satellite dataset of precipitation, covering the majority of the globe and providing data even in areas without rain gauges.

The generalised extreme value (GEV) distribution is fitted to a total of 4.32 million cells at 25 durations. The Ailliot et al. 2011 CM1 method is used, combining the strength of L-moment and maximum-likelihood estimators for best performance at small sample sizes. L-moments and the shape parameter κ are regionalised to improve parameter estimation, and sample plots are presented at the global scale.

XRain estimates are compared with those from USA, UK, Australia and New Zealand to demonstrate spatial variability and the variability between different durations and frequencies. Patterns are replicated reasonably well, with the ratio between XRain depths and depth from the local dataset not varying dramatically. However it is recommended that predictions are calibrated against available local data wherever possible.

XRain Report EH1
Revision 5, November 2022
Dr Cameron Oliver

Contents

1 Overview

Extreme precipitation statistics are estimates of the depth or intensity of precipitation that will occur at a certain frequency, and are used for modelling the flooding that might occur at a location; estimating volume, depth, velocity and other parameters. This information can in turn be used to evaluate flood risk, to set floor levels for new buildings, to design stormwater infrastructure such as pipes, culverts or detention basins, and to test whether proposed flood protection/mitigation works like dykes (levees) or groynes will be effective. It can also be used to test the design of roads or bridges or to evaluate the performance of dams in flood events.

Extreme precipitation is sometimes known as *design rainfall*, *precipitation frequency*, *intensity-duration-frequency*, *depth-duration-frequency* or *high intensity* precipitation. The terms intensity-duration-frequency (IDF) and depth-duration-frequency (DDF) also describe the tabular format that this data is generally presented in, depending on whether average intensity or total depth is listed.

The frequency that a certain level of precipitation will occur at is expressed in terms of:

- the **annual exceedance probability** (AEP), which is the probability that an event of that size or greater will occur in a given year, *or*
- the **average recurrence interval** (ARI), which is the average time period between events of that size or greater, and is also known as the return period.

As larger drainage basins[1] are affected by rainfall over a longer period of time than smaller drainage basins, duration is an important part of such an analysis.

Generally, extreme precipitation statistics are derived from long-term rain gauge records. Rain gauges *directly* measure the precipitation at a certain point location; if they are installed appropriately and cover a sufficiently long period of time they can provide excellent data. However, estimating precipitation between rain gauges can be a difficult process; relying on assumptions about orographic effects, etc. There are many parts of the world that are physically distant from available rain gauges, presenting a formidable challenge for flood protection and management projects.

The goal of this work was to derive extreme precipitation statistics from a satellite-measured dataset of historical precipitation made by the Global Precipitation Measurement (GPM) mission, a joint project between NASA and JAXA. The dataset, known as GPM_3IMERGHH_06 (Huffman et al. 2019)[2] covers the majority of the globe, providing data even in areas without rain gauges.

This work analysed precipitation from 2001 to 2020, providing a baseline of historical conditions. To allow for climate change, users should apply local guidance or IPCC AR6 (Intergovernmental Panel on Climate Change Sixth Assessment Report) projections at interactive-atlas.ipcc.ch.

The resulting DDF/IDF data is available for purchase from xrain.info/data.

[1] Also known as *watersheds* or *catchments*

[2] GPM IMERG (Integrated Multi-satellitE Retrievals for GPM) Final Precipitation L3 Half Hourly 0.1 degree x 0.1 degree V06B

2 Source Dataset

The GPM_3IMERGHH_06 (Huffman et al. 2019) dataset supplies a calibrated precipitation field ("precipitationCal") in units of mm/hr. This data is derived from measurements made by passive microwave (PMW) sensors on a constellation of satellites orbiting the earth, and is calibrated against monthly precipitation totals taken from over 79,000 rain gauge stations across the world. Calibration rain gauge data is supplied by the Global Precipitation Climatology Centre (GPCC).

The dataset:

- Has a temporal resolution (i.e. time step) of 30 minutes[3]
- Begins 1 June 2000, but for this analysis full years of data are used, from 2001 to 2020.
- Has near-complete temporal coverage between 60° N and 60° S
- Uses the WGS84 coordinate system (EPSG 4326) with a spatial resolution of 0.1° by 0.1°; roughly 11 km by 11 km at the equator and 6 km by 11 km at ± 60° latitude.

This resolution equates to 3600 cells (pixels) wide by 1200 cells high between 60° N and 60° S; a total of 4.32 million cells. Figure 1 plots mean annual depth between 60° N and 60° S.

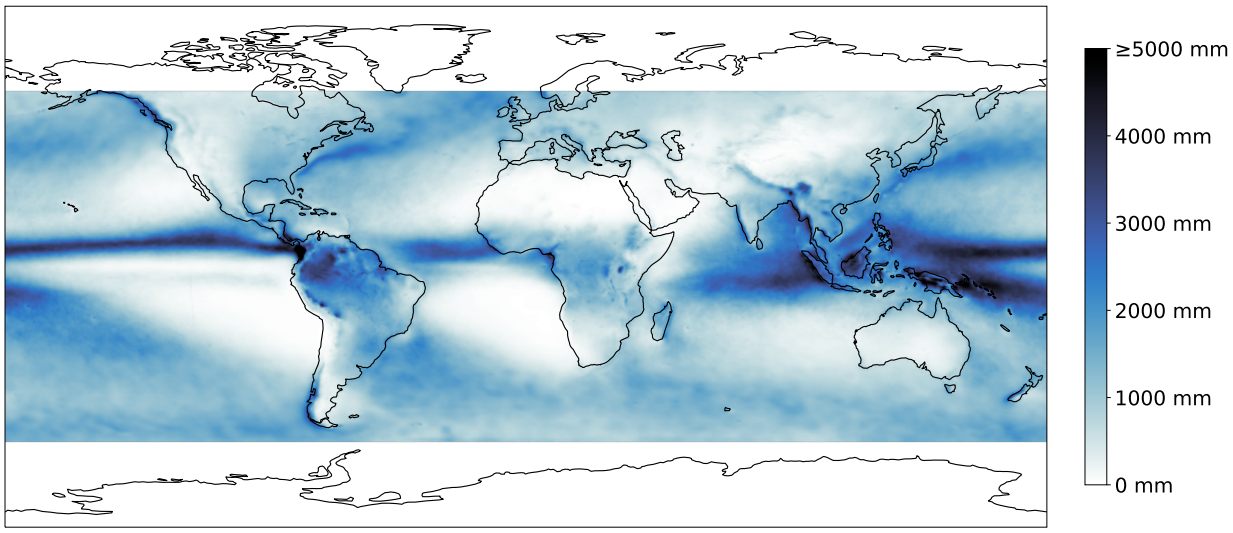

Figure 1: Mean annual depth

3 Approach

The objective of this work was to estimate precipitation at various probabilities of occurrence, particularly at low AEP or high ARI values (such as the 1% AEP).

The greatest runoff produced from small drainage basins is driven by short but intense precipitation, while the greatest runoff from large drainage basins is driven by longer sustained precipitation. Hydrologically this is represented by the **lag time** or **time of concentration**

[3]While the data is presented with a uniform time step, it is based on periodic near-instantaneous measurements as satellites orbit the earth.

parameters (Woodward 2010). Therefore in order to be widely applicable, this analysis of extreme precipitation was conducted at a wide range of durations; specifically:

> 1 hr, 1.5 hrs, 2 hrs, 2.5 hrs, 3 hrs, 4 hrs, 5 hrs, 6 hrs, 8 hrs, 10 hrs, 12 hrs, 16 hrs, 20 hrs, 24 hrs, 30 hrs, 36 hrs, 48 hrs (2 days), 72 hrs (3 days), 96 hrs (4 days), 168 hrs (1 week), 336 hrs (2 weeks), 672 hrs (4 weeks), 1008 hrs (6 weeks), 2016 hrs (12 weeks), and 3024 hrs (18 weeks).

Of note, the 0.5 hour duration was excluded, because a 0.5 hour time step does not adequately resolve a 0.5 hour event (if the event starts and finishes between time steps it may result in significantly lower depths than it had in reality). This is analogous to the Nyquist frequency in signal processing.

Historically the peak over threshold (POT) method has been used to derive average recurrence intervals (ARIs) while the annual maxima method has been used to derive annual exceedance probabilities (AEPs). The peak over threshold method, also known as the partial duration series, considers events above a certain threshold. The major difficulties with this method are ensuring the independence of events and choosing an appropriate threshold value (Bezak et al. 2014). By contrast the annual maxima method simply identifies the largest event in each year, with no need for a threshold.

This analysis was carried out using the annual maxima method, and in terms of annual exceedance probability. Conversion to average recurrence interval is done as required, using the inverse of Langbein's formula (Langbein 1949); i.e. $\text{ARI} = -1/\ln(1 - \text{AEP})$. This formula is approximately equal to the commonly-used equation $\text{ARI} = 1/\text{AEP}$ above an ARI of 10 years (Figure 2).

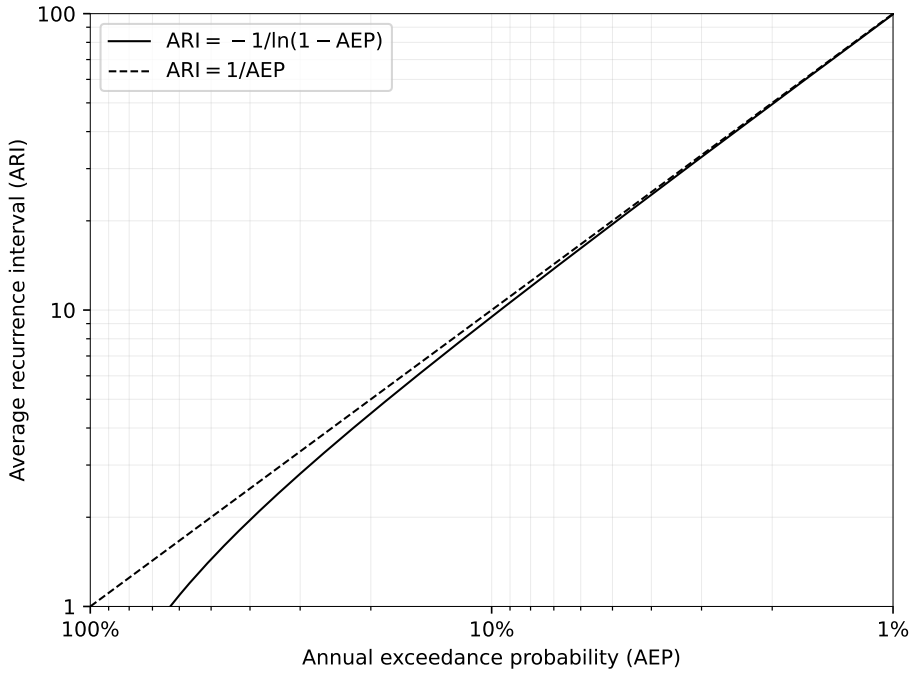

Figure 2: Difference between Langbein 1949 formula and 1/AEP

At every location (pixel), the *moving total depth* was calculated for each of the durations listed above. The largest event in each year was then identified.

Fisher and Tippett 1928 showed that there are three possible limiting distributions for extremes, which are now known as the Gumbel (type 1), Fréchet (type 2) and reversed Weibull (type 3). The **generalised extreme value (GEV)** distribution (von Mises 1936; frequently attributed to Jenkinson 1955) unifies these three distributions into a single expression, and has been used to analyse precipitation across the globe (Papalexiou and Koutsoyiannis 2013). For this work, we fitted the GEV distribution to annual maxima depths at each location and duration, giving the ability to estimate precipitation at any arbitrary AEP or ARI.

This statistical analysis implicitly makes the assumption that climatic conditions have not changed over the period in question—a "stationary" climate. This is not true, for at least two reasons:

1. Climate change: there is strong consensus that global surface temperatures are increasing, leading to more frequent weather extremes, including precipitation extremes (droughts and heavy rainfall).
2. Long-term (multi-decade) climate oscillations such as the Atlantic Multidecadal Oscillation and the Indian Ocean Dipole can lead to increases in precipitation in some places and decreases in others. These effects will invariably be seen in extreme precipitation events, and therefore will influence the extreme precipitation statistics calculated from the GPM_3IMERGHH_06 dataset.

Users will need to account for these as necessary in their use of the data. With respect to climate change, users should use local guidance or IPCC AR6 (Intergovernmental Panel on Climate Change Sixth Assessment Report) projections at interactive-atlas.ipcc.ch.

4 Fitting Procedure

The generalised extreme value (GEV) distribution, introduced above, is a robust and flexible distribution for modelling extreme values.

The GEV distribution has three parameters, $\sigma > 0$ (scale), μ (location) and κ (shape). The cumulative distribution function is given by

$$F(z) = \begin{cases} e^{-(1-\kappa z)^{1/\kappa}} & \kappa \neq 0 \\ e^{-e^{-z}} & \kappa = 0 \end{cases} \tag{1}$$

where

$$z = \frac{x - \mu}{\sigma} \tag{2}$$

Translating this to more familiar terms, the annual exceedance probability AEP of an event of size x is

$$\text{AEP} = 1 - F(z) = 1 - \begin{cases} e^{-(1-\kappa z)^{1/\kappa}} & \kappa \neq 0 \\ e^{-e^{-z}} & \kappa = 0 \end{cases} \tag{3}$$

The inverse is

$$x = \begin{cases} \mu + \sigma \dfrac{1 - (-ln(1 - \text{AEP}))^{\kappa}}{\kappa} & \kappa \neq 0 \\ \mu - \sigma ln(-ln(1 - \text{AEP})) & \kappa = 0 \end{cases} \tag{4}$$

When $\kappa = 0$, the GEV distribution reduces to the two parameter Gumbel (type 1). $\kappa < 0$ corresponds to a heavy-tail Fréchet distribution (type 2) with a lower bound of $\sigma/\kappa + \mu$, and $\kappa > 0$ to a light-tail Weibull distribution (type 3) with an upper bound of $\sigma/\kappa + \mu$.

At low AEP values (such as the 1% AEP), the GEV distribution is particularly sensitive to the κ (shape) parameter.

Three methods are commonly used for fitting the GEV distribution to annual maxima samples:

- Method of moments (MOM; Chebyshev 1887)
- Maximum-likelihood estimators (MLE; Prescott and Walden 1980), where the parameters μ, σ and κ are those that maximise the likelihood function (or the log of the likelihood function), *and*
- L-moment (LM) estimators (Hosking 1990), equivalent to probability-weighted moment (PWM) estimators

Hosking et al. 1985 found that for small samples, MLEs can be unstable, and while LM estimators produced biased estimates, they were preferable to maximum likelihood estimators because they resulted in smaller variances. Madsen et al. 1997 showed that with small samples the conventional MOM estimators were more accurate than either MLE or LM estimators. They showed that MLEs are preferable only when $\kappa > 0.3$ and the sample size n exceeds 50.

Morrison and Smith 2002 developed procedures that combined MLE and LM methods. These mixed methods gave reduced variance compared to the MLE estimator, and reduced bias compared to the LM estimator. They paid particular attention to the shape parameter, which influences the upper tail of the frequency distribution.

Ailliot et al. 2011 developed mixed MLE and LM methods that constrained the shape parameter κ between -0.5 and 0.5. Note that in hydrology it is often assumed that κ lies in a more restrictive range such as between -0.3 and 0.3 (for example see Hosking et al. 1985). The Ailliot et al. 2011 CM1 method involves maximising the log-likelihood function $\ln L(\theta)$ as a function of κ after taking μ and σ from L-moment estimators. It is equivalent to the Morrison and Smith 2002 MIX2 method plus the constraint $-0.5 < \kappa < 0.5$.

The log-likelihood of a random sample $x_1, ..., x_n$ drawn from a GEV distribution with $\kappa \neq 0$ is given by

$$\ln L(\theta) = -n \ln \sigma - \sum_{i=0}^{n} \left(1 - \frac{\kappa(x_i - \mu)}{\sigma}\right)^{1/\kappa} + \left(\frac{1}{\kappa} - 1\right) \sum_{i=0}^{n} \ln\left(1 - \frac{\kappa(x_i - \mu)}{\sigma}\right) \tag{5}$$

where the term $\kappa(x_i - \mu)$ must be less than or equal to σ for any sample x_i, and:

$$\sigma = \begin{cases} \frac{\lambda_2 \kappa}{(1-2^{-\kappa})\Gamma(1+\kappa)} > 0 & \kappa \neq 0 \\ \lambda_2 / \log(2) > 0 & \kappa = 0 \end{cases} \tag{6}$$

$$\mu = \begin{cases} \lambda_1 - \frac{\sigma}{\kappa}(1 - \Gamma(1+\kappa)) & \kappa \neq 0 \\ \lambda_1 - \gamma\sigma & \kappa = 0 \end{cases} \tag{7}$$

where γ is the Euler-Mascheroni constant.

The terms λ_1 and λ_2 are the first and second "unbiased" sample L-moments calculated using Hosking's `samlmu` method (as described in Hosking 1990 and implemented in version 2.8 of the r package lmom by Hosking, March 2019). As per Hosking 1990, λ_1 and λ_2 may be regarded as measures of location and scale respectively.

This work employs the Ailliot et al. 2011 CM1 method but with L-moments and κ first regionalised (see following section).

It is worth noting that L-moment based estimators do not require any information on the AEP of each annual maxima (known as the "plotting position"). However we must assign AEP values if we wish to plot maxima against the fitted GEV curve to inspect results. For this purpose the distribution-free Weibull 1939 method was used[4]. Expressed in terms of AEP the Weibull method states that for N ranked samples, AEP $= 1 - m/(N+1)$, where m is the rank, with $m = 1$ for the smallest value and $m = N$ for the largest value.

5 Regionalisation

With 20 years of historical data (1 Jan 2001 to 31 Dec 2020), the annual maxima method provides 20 values. As alluded to above, fitting the GEV distribution to small sample sizes such as this is challenging. The various fitting methods discussed above assume that samples are representative of long-term climate, but this will not always be the case. Samples may represent unusually dry or unusually wet years, or they may include extremely rare events (a 5000 year ARI event, for instance). A straightforward fit of the GEV to annual maxima may result in depth predictions for one cell that are significantly different from an immediately adjacent cell with essentially the same climate.

Regionalisation is a standard practice for improving the estimation of extreme event distributions by pooling samples from sites with short records. The index-frequency method, first proposed by Dalrymple 1960, involves dividing annual maxima from each site by a scaling factor (the index variable) and fitting a distribution to the combined normalised samples.

This method assumes that:

- once annual maxima have been appropriately normalised, the underlying distribution at each site is identical, *and*
- records are mutually independent (not including multiple samples of the same event, for instance).

[4] See Makkonen et al. 2013 for justification of the use of the Weibull method

The second may be valid if the time periods of records at each site do not overlap, or if sites are sufficiently distant from each other that they are not affected by the same weather events. However the first, while difficult to prove, becomes increasingly *unlikely* as the distance between each site increases.

Nevertheless, it has been demonstrated by Hosking and Wallis 1988 that while the presence of inter-site dependencies decreases accuracy of flood quantile estimates, it does not lead to bias. They state "Even when both heterogeneity [inequality of the flood frequency distributions in the region] and intersite dependence are present and the form of the flood frequency distribution is misspecified, regional flood frequency analysis is more accurate than at-site analysis."

In this study, the index variable was taken as the median annual precipitation for each cell. The median was used in preference to the mean because it is not usually affected by the presence of outliers (Reed et al. 1999, Carey-Smith et al. 2018).

We can demonstrate empirically that when fitting the GEV distribution to a set of samples normalised by the index value i:

- The κ value derived is the same value as is derived from the un-normalised samples:

$$\kappa(\text{maxima}/i) = \kappa(\text{maxima})$$

- Other parameters are related as a function of $1/i$:

$$\lambda_1(\text{maxima}/i) = \lambda_1(\text{maxima})/i$$

$$\lambda_2(\text{maxima}/i) = \lambda_2(\text{maxima})/i$$

$$\mu(\text{maxima}/i) = \mu(\text{maxima})/i$$

$$\sigma(\text{maxima}/i) = \sigma(\text{maxima})/i$$

Two regionalisation processes were carried out for this study. The first was to regionalise the Hosking L-moments λ_1 and λ_2 by pooling normalised annual maxima from a selection of neighbouring cells. The second was to independently regionalise the κ (shape) parameter using the Ailliot et al. 2011 CM1 method by maximising the log-likelihood function (equation 5 with the constraint $-0.5 < \kappa < 0.5$) on pooled normalised annual maxima.

Figure 3 plots regionalised λ_1 (location) for 1 hour, 1 day and 4 weeks. In general terms a higher λ_1 value corresponds to higher extreme precipitation. Of interest:

- The highest values are generally seen over the ocean within the tropics (23° S to 23° N), while the lowest values are seen over North Africa and to the west of both South America and Southern Africa.
- The Philippines Sea and South China Sea are particularly dominant in the 1 day image, while at 4 weeks duration the western coastlines of Myanmar and India are particularly dominant.

Figure 4 plots regionalised κ (shape) for 1 hour, 1 day and 4 weeks. Observations include:

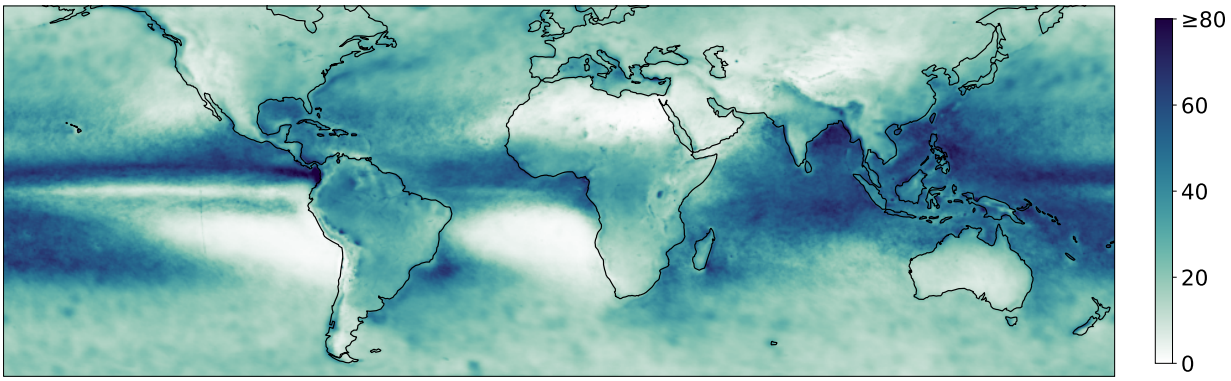

(a) 1 hour

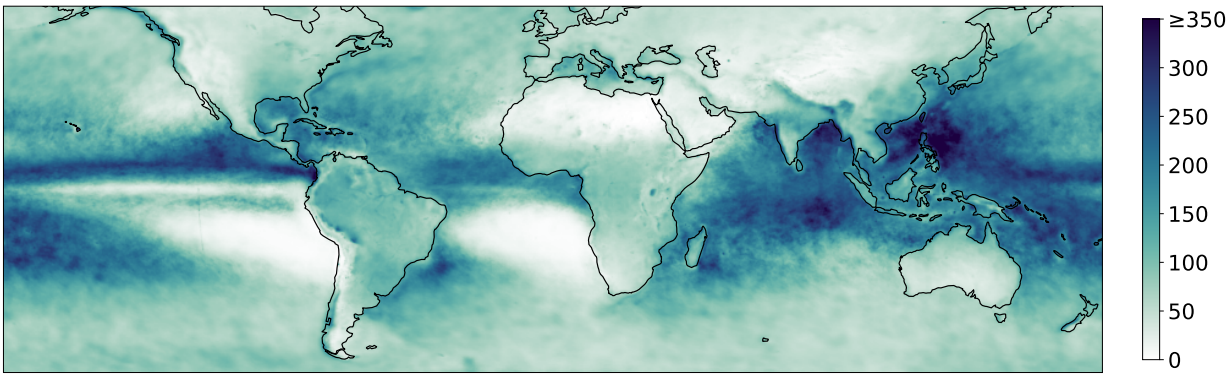

(b) 24 hours (1 day)

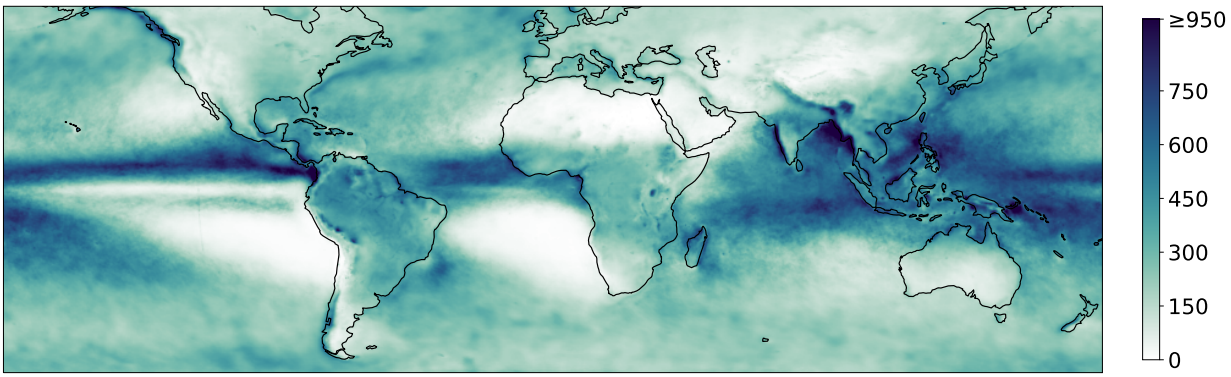

(c) 672 hours (4 weeks)

Figure 3: λ_1 (first L-moment; location)

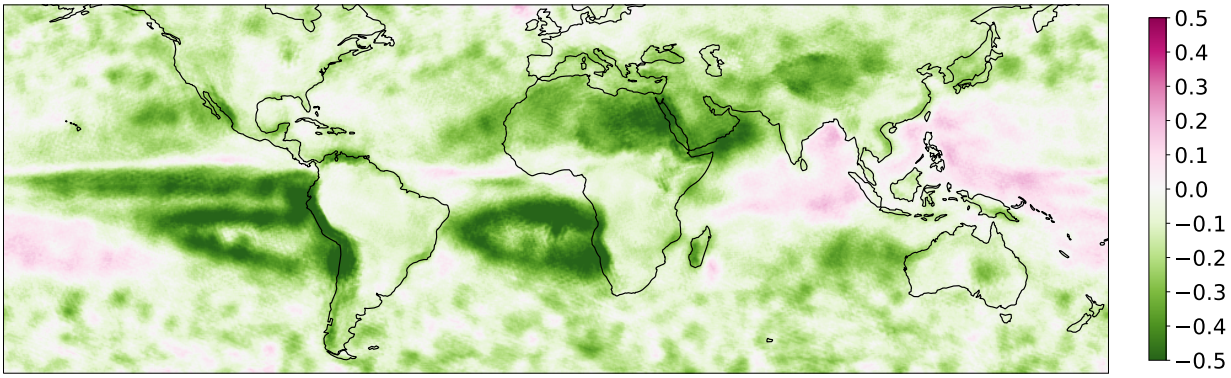

(a) 1 hour

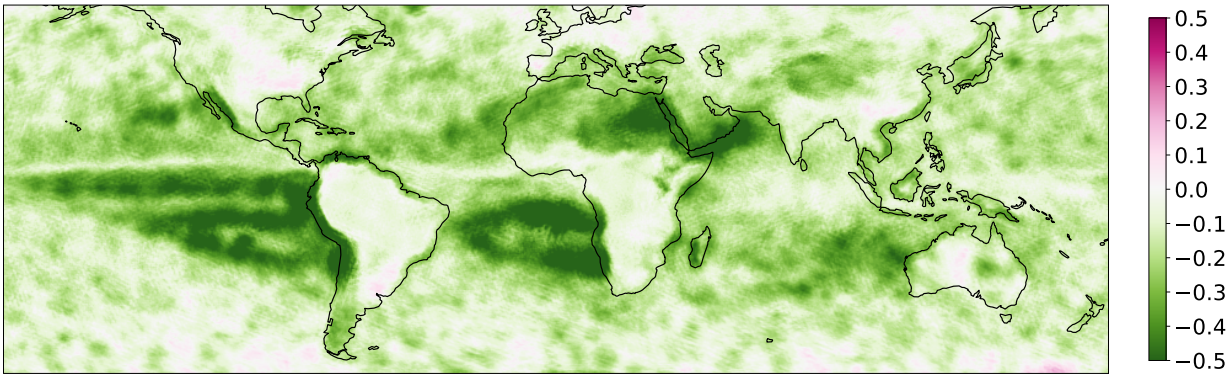

(b) 24 hours (1 day)

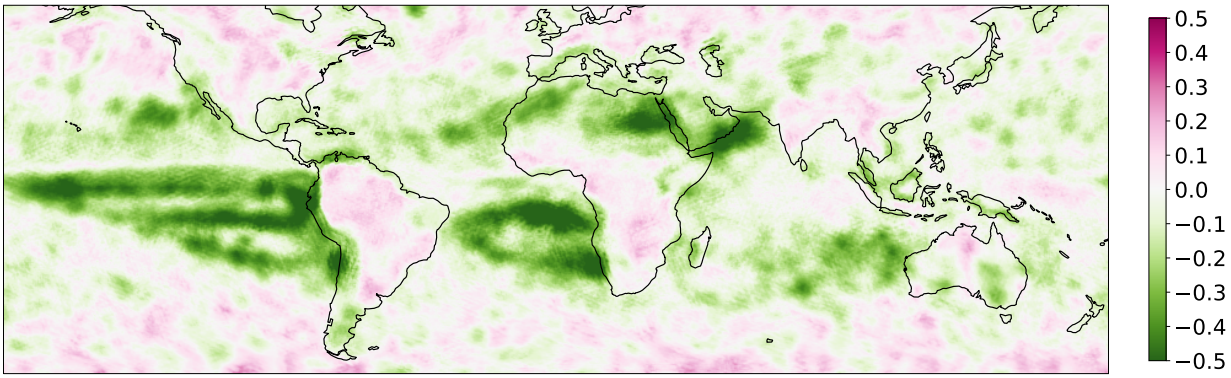

(c) 672 hours (4 weeks)

Figure 4: κ (shape parameter)

- Across all images, negative κ values are more common than positive values (in fact the highest value in these images is 0.36; seen at 60° S in the 4 week image).
- At 1 1 hour, positive values are seen in coastal areas surrounding Southeast Asia and to the south of India.
- At 4 weeks, positive κ values are seen across many continental regions, including in North America, South America and Southern Africa.

σ and μ were subsequently calculated by substituting the regionalised κ, λ_1 and λ_2 values into equations 6 and 7.

Figure 5 plots the resulting 1% AEP depth at 1 hour, 1 day and 4 weeks.

6 Validation

Because XRain is based on remotely-sensed precipitation data, it is by nature less accurate than data derived from rain gauges. This means that if extreme statistics based on rain gauge data are available for a site, this is likely to be the best choice. However there are many parts of the world where appropriate long-term rain gauges are at a considerable distance away, and where extrapolation from these is difficult.

It is helpful to compare XRain predictions to those from well-serviced areas, in order to understand the nature and magnitude of differences. This can then guide the user in calibrating against local data in other parts of the world.

6.1 Country-scale

For this exercise we use the NOAA Atlas 14 Precipitation Frequency dataset of extreme precipitation across southeastern United States (Bonnin et al. 2006, Perica et al. 2013).

Figure 6 plots the percentage difference between XRain depths and NOAA Atlas 14 depths[5] at the 1% AEP. At the 1 hour duration, XRain under-predicts depth by approximately 40% in most of the region. At 1 day and 1 week the differences are generally within 20%, but exceed 50% in some coastal fringes of Florida and Louisiana.

6.2 Site specific

For this exercise four cities were selected where extreme precipitation data is readily available (Table 1)[6].

Figure 7 plots depth vs. AEP at the 24 hour duration. On the whole patterns are replicated reasonably well, with the ratio between XRain depths and depth from the local dataset not varying dramatically.

Figure 8 plots depth vs. duration at 1% AEP. Again patterns are replicated reasonably well, with the ratio between XRain depths and depth from the local dataset not varying dramatically.

[5] (XRain depth minus NOAA depth) divided by NOAA depth

[6] For Washington DC, data was obtained at the location of the United States Capitol. For other cities, data was obtained at the location of their respective parliament buildings

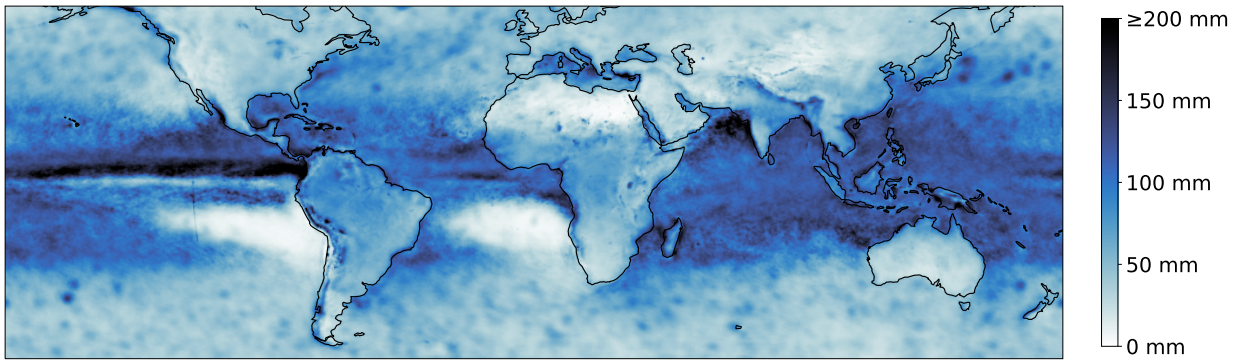

(a) 1 hour

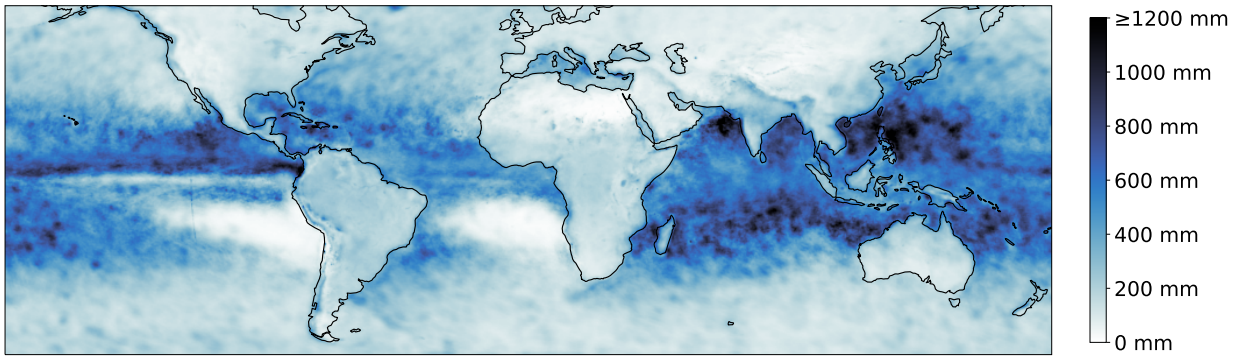

(b) 24 hours (1 day)

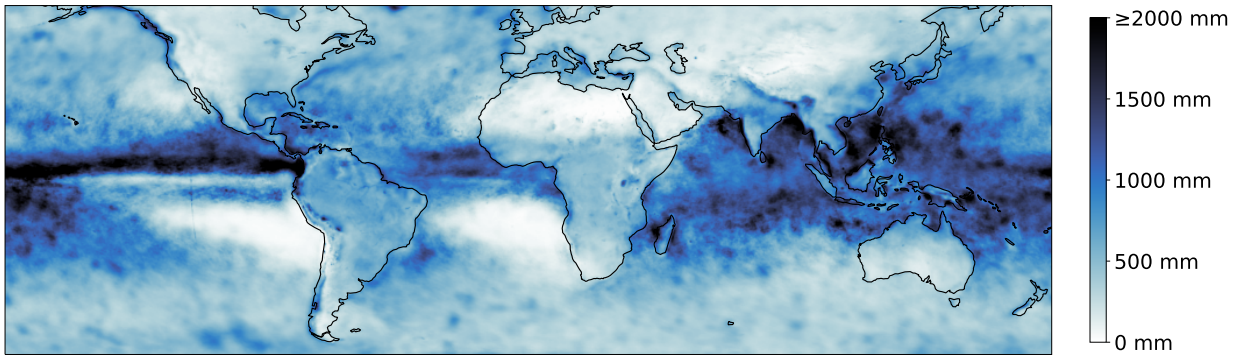

(c) 672 hours (4 weeks)

Figure 5: 1% AEP depth

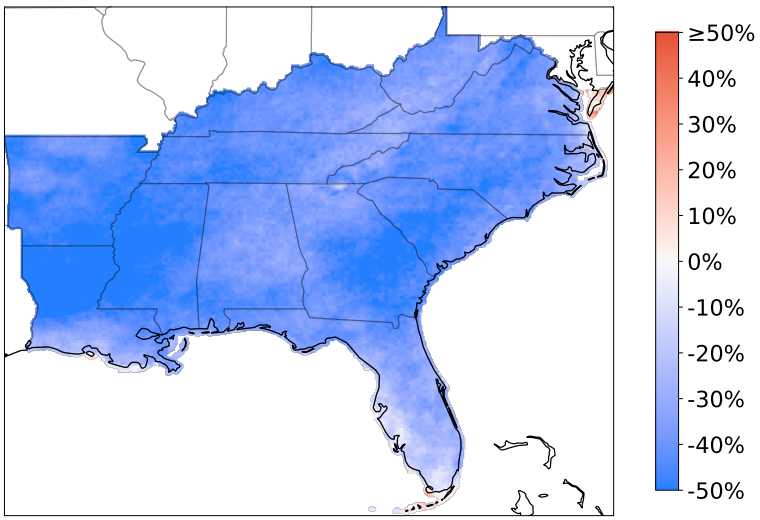

(a) 1 hour

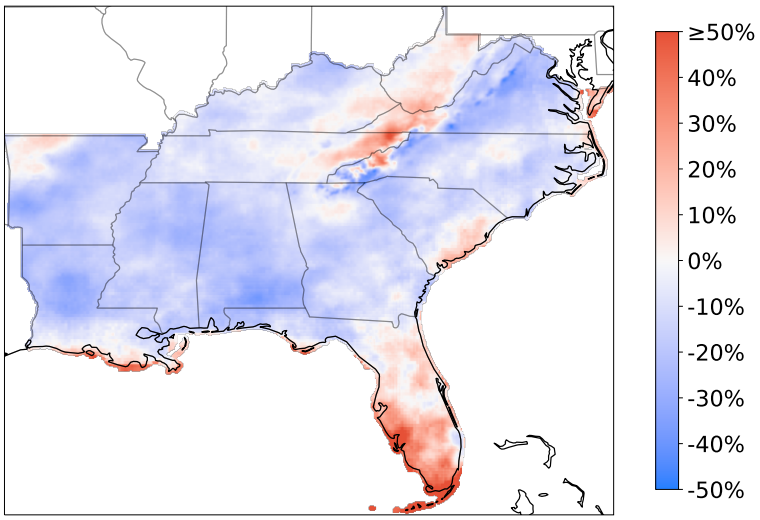

(b) 24 hours (1 day)

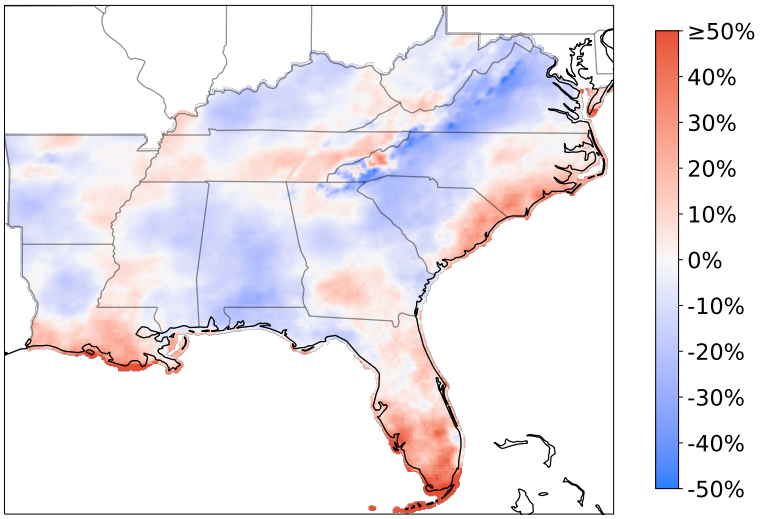

(c) 168 hours (1 week)

Figure 6: Percentage difference between XRain depths and NOAA Atlas 14 depths, south-eastern states

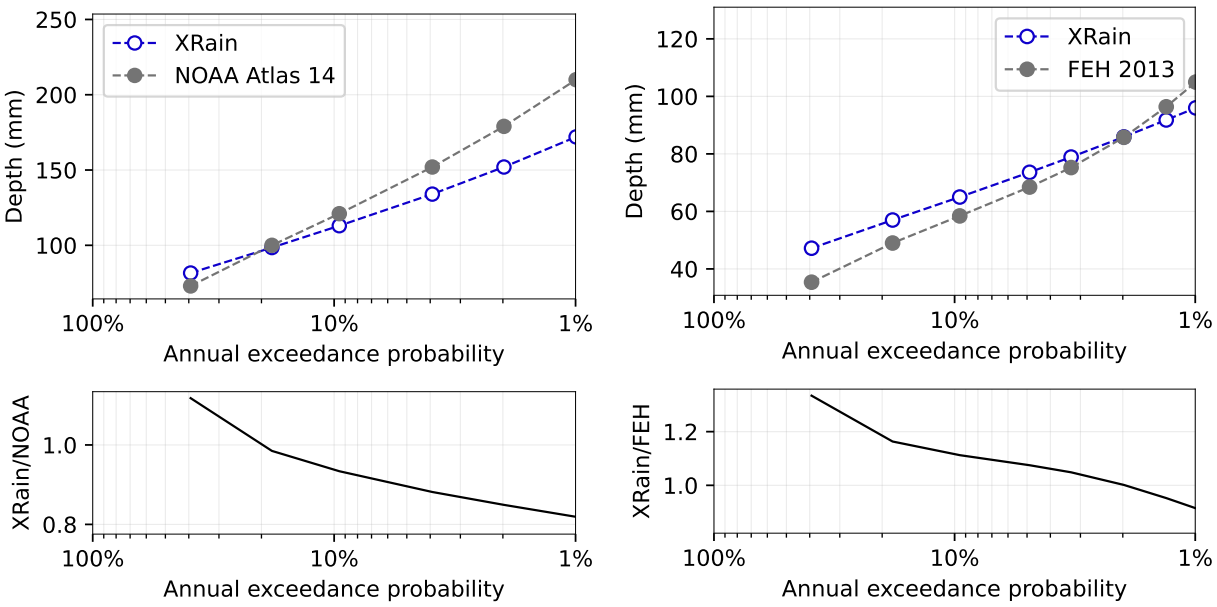

(a) Washington DC

(b) London

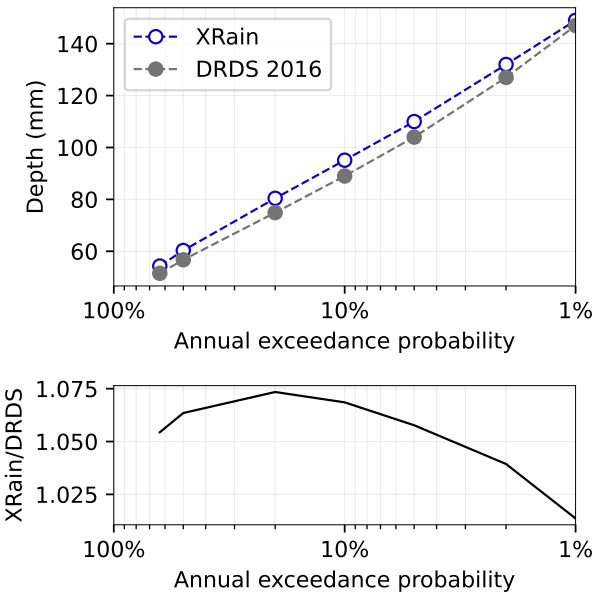

(c) Canberra

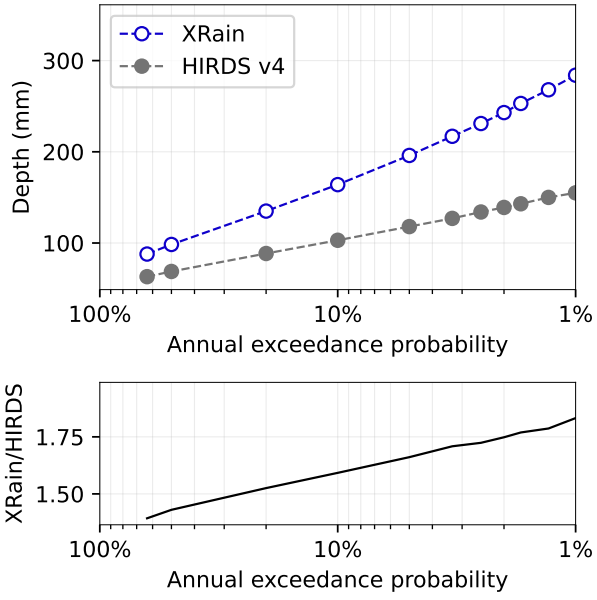

(d) Wellington

Figure 7: Depth vs. AEP at 24 hour duration

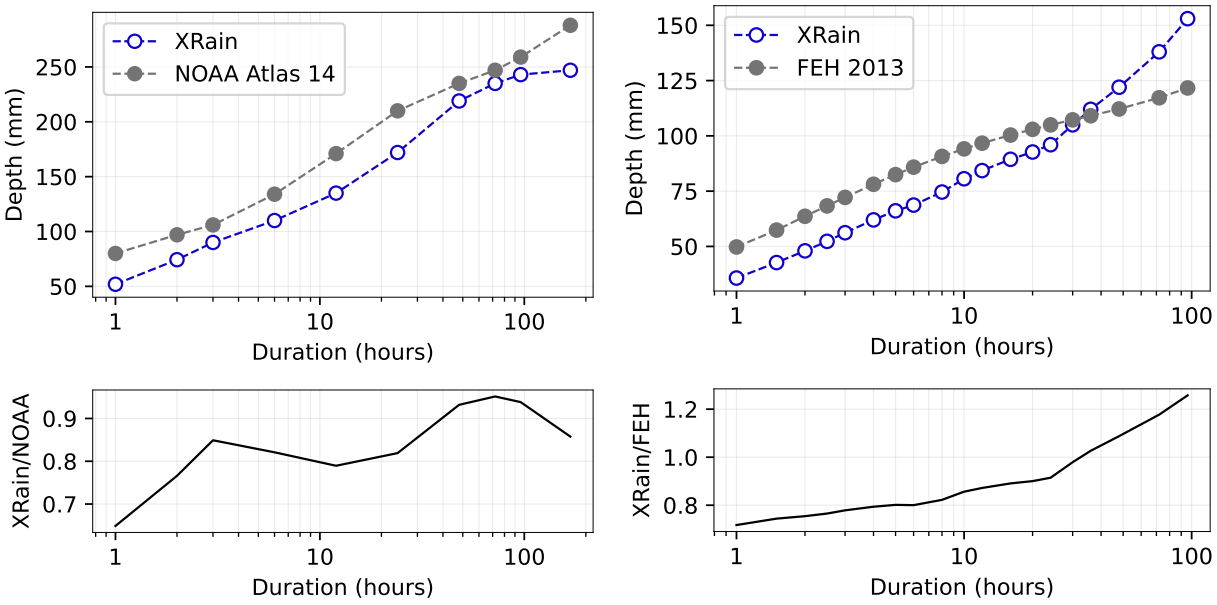

(a) Washington DC

(b) London

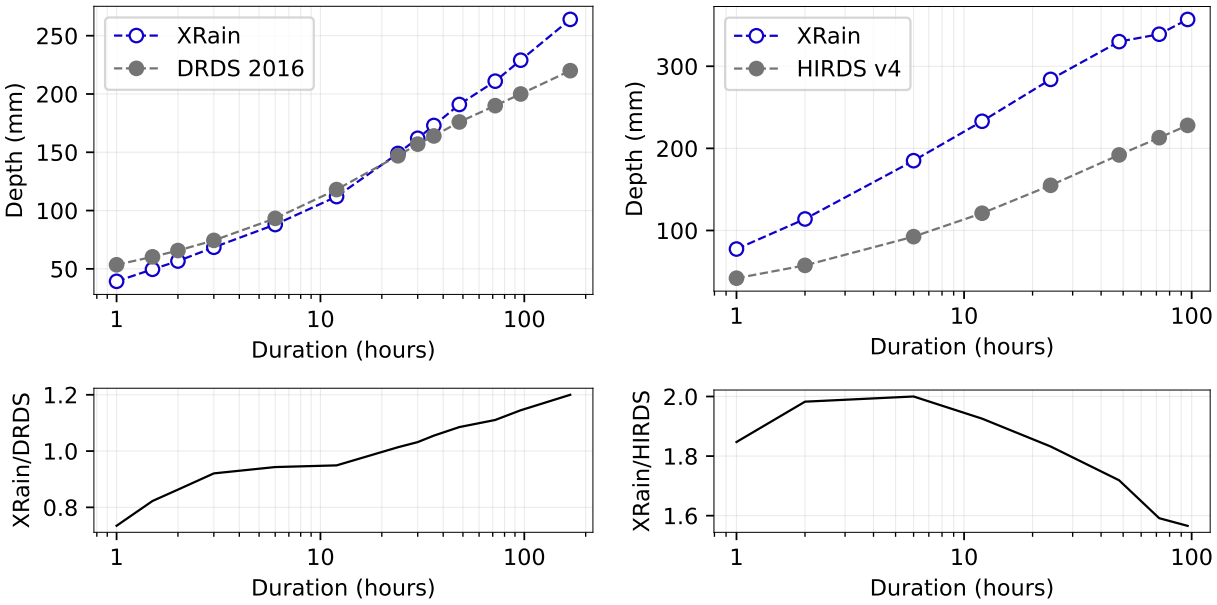

(c) Canberra

(d) Wellington

Figure 8: Depth vs. duration at 1% AEP

Country	Location	Data source
United States of America	Washington DC	NOAA Atlas 14 Precipitation Frequency Data Server (multiple volumes)
United Kingdom	London	FEH 2013: Flood Estimation Handbook Web Service (Stewart et al. 2010)
Australia	Canberra	DRDS 2016: Design Rainfall Data System 2016 (Green et al. 2015)
New Zealand	Wellington	HIRDS v4: High Intensity Rainfall Design System v4 (Carey-Smith et al. 2018)

Table 1: Validation sites and data sources

6.3 Recommended calibration procedure

If *partial* extreme data for the location of interest is available from a third party source, then it is recommended that XRain data is scaled to match the available data. For example, if 24 hour depths are provided for the 20 year ARI event, then depths for other durations can be estimated by factoring XRain estimates by the ratio between the provided 24 hour depth and the XRain 24 hour depth.

If extreme data is not available at the location of interest but is available at a *neighbouring site*, we recommend:

- Obtain XRain estimates at the neighbouring site for the same durations and AEP or ARI values. Calculate the ratio between supplied estimates and XRain estimates for each duration and AEP or ARI.
- Obtain XRain estimates at the location of interest and multiply these by the ratios calculated at the neighbouring site.

In both scenarios it may be advisable to add a factor of safety to estimated values.

7 DDF/IDF tables

By thought experiment, we can deduce that DDF/IDF tables have the following properties:

- As AEP decreases (or ARI increases), depth or intensity must increase or stay the same (rarer events cannot have less rainfall):

$$\frac{\text{dDepth}}{\text{dAEP}} \geq 0 \tag{8}$$

- As duration increases, total depth must increase or stay the same (we are including a longer time period so cannot have less precipitation):

$$\frac{\text{dDepth}}{\text{dDuration}} \geq 0 \tag{9}$$

- As duration increases the average intensity must decrease or stay the same:

$$\frac{\text{dIntensity}}{\text{dDuration}} \leq 0 \tag{10}$$

The first of these properties is satisfied by the condition in equation 6 that $\sigma > 0$. However, because the GEV curve is fitted to annual maxima at each duration independently, the conditions described by equations 9 and 10 are sometimes violated; particularly at lower AEP values (higher ARI). The approach taken by this work was to enforce these conditions as a post-processing step. In other words, for a given AEP or ARI, as we iterate through durations from shortest to longest:

- if GEV depth is less the depth calculated at the previous duration, we use the depth at that previous duration instead, *and*
- if the equivalent average intensity is greater than the average intensity calculated at the previous duration, we use that previous intensity instead, and then multiply it by the current duration to get depth.

8 Conclusion

Historical extreme precipitation statistics have have calculated from a NASA/JAXA dataset of historical precipitation known as GPM_3IMERGHH_06. This dataset is made from satellite measurements and calibrated against monthly precipitation totals taken from over 79,000 rain gauge stations across the world.

Predictions from the resulting product, known as XRain and available from xrain.info/data, have been compared against those in the USA, UK, Australia and New Zealand. Patterns are replicated reasonably well, with the ratio between XRain depths and depth from the local dataset not varying dramatically. However it is recommended that predictions are calibrated against available local data wherever possible.

This work analysed precipitation from 2001 to 2020, providing a baseline of historical conditions. To allow for climate change, users should apply local guidance or IPCC AR6 projections.

References

Ailliot, Pierre, Thompson, Craig, and Thomson, Peter (May 2011). "Mixed methods for fitting the GEV distribution". In: *Water Resources Research* 47.5. ISSN: 00431397. DOI: 10.1029/2010WR009417.

Bezak, Nejc, Brilly, Mitja, and Šraj, Mojca (May 4, 2014). "Comparison between the peaks-over-threshold method and the annual maximum method for flood frequency analysis". In: *Hydrological Sciences Journal* 59.5, pp. 959–977. ISSN: 0262-6667, 2150-3435. DOI: 10.1080/02626667.2013.831174.

Bonnin, Geoffrey M., Martin, Deborah, Lin, Bingzhang, Parzybok, Tye, Yekta, Michael, and Riley, David (2006). *Precipitation-Frequency Atlas of the United States Volume 2 Version 3.0: Delaware, District of Columbia, Illinois, Indiana, Kentucky, Maryland, New Jersey, North Carolina, Ohio, Pennsylvania, South Carolina, Tennessee, Virginia, West Virginia*. Silver Spring, Maryland: U.S. Department of Commerce National Oceanic and Atmospheric Administration National Weather Service.

Carey-Smith, Trevor, Henderson, Roddy, and Singh, Shailesh (Aug. 2018). *High Intensity Rainfall Design System Version 4*. 2018022CH. Prepared for Envirolink. URL: https://niwa.co.nz/sites/niwa.co.nz/files/2018022CH_HIRDSv4_Final.pdf.

Chebyshev, Pafnuty Lvovich (1887). "О двух теоремах относительно вероятностей (On two theorems concerning probabilities)". In: *Приложение к LV тому записок императорской академии наук (Appendix to Volume LV of the Notes of the Imperial Academy of Sciences), No. 6*.

Dalrymple, Tate (1960). *Flood-frequency analysis*. Geological Survey Water-Supply Paper 1543-A. U.S. Department of the Interior.

Fisher, R. A. and Tippett, L. H. C. (Apr. 1928). "Limiting forms of the frequency distribution of the largest or smallest member of a sample". In: *Mathematical Proceedings of the Cambridge Philosophical Society* 24.2, pp. 180–190. ISSN: 0305-0041, 1469-8064. DOI: 10.1017/S0305004100015681.

Green, Janice, Beesley, Catherine, The, Cynthia, and Podger, Scott (Jan. 2015). "New Design Rainfalls for Australia". In: *36th Hydrology and Water Resources Symposium: The Art and Science of Water*. Hobart, Tasmania: Engineers Australia.

Hosking, J. R. M. (Sept. 1990). "L-Moments: Analysis and Estimation of Distributions Using Linear Combinations of Order Statistics". In: *Journal of the Royal Statistical Society: Series B (Methodological)* 52.1, pp. 105–124. ISSN: 00359246. DOI: 10.1111/j.2517-6161.1990.tb01775.x.

Hosking, J. R. M. and Wallis, J. R. (Apr. 1988). "The effect of intersite dependence on regional flood frequency analysis". In: *Water Resources Research* 24.4, pp. 588–600. ISSN: 00431397. DOI: 10.1029/WR024i004p00588.

Hosking, J. R. M., Wallis, J. R., and Wood, E. F. (Aug. 1985). "Estimation of the Generalized Extreme-Value Distribution by the Method of Probability-Weighted Moments". In: *Technometrics* 27.3, pp. 251–261. ISSN: 0040-1706, 1537-2723. DOI: 10.1080/00401706.1985.10488049.

Huffman, G.J., Stocker, E.F., Bolvin, D.T., Nelkin, E.J., and Tan, J. (2019). *GPM IMERG Final Precipitation L3 Half Hourly 0.1 degree x 0.1 degree V06*. Type: dataset. DOI: 10.5067/GPM/IMERG/3B-HH/06.

Jenkinson, A. F. (Apr. 1955). "The frequency distribution of the annual maximum (or minimum) values of meteorological elements". In: *Quarterly Journal of the Royal Meteorological Society* 81.348, pp. 158–171. ISSN: 00359009, 1477870X. DOI: 10.1002/qj.49708134804.

Langbein, W. B. (1949). "Annual floods and the partial-duration flood series". In: *Transactions, American Geophysical Union* 30.6, p. 879. ISSN: 0002-8606. DOI: 10.1029/TR030i006p00879.

Madsen, Henrik, Rasmussen, Peter F., and Rosbjerg, Dan (Apr. 1997). "Comparison of annual maximum series and partial duration series methods for modeling extreme hydrologic events: 1. At-site modeling". In: *Water Resources Research* 33.4, pp. 747–757. ISSN: 00431397. DOI: 10.1029/96WR03848.

Makkonen, Lasse, Pajari, Matti, and Tikanmäki, Maria (Sept. 2013). "Discussion on "Plotting positions for fitting distributions and extreme value analysis"". In: *Canadian Journal of Civil Engineering* 40.9, pp. 927–929. ISSN: 0315-1468, 1208-6029. DOI: 10.1139/cjce-2013-0227. URL: http://www.nrcresearchpress.com/doi/10.1139/cjce-2013-0227 (visited on 05/29/2022).

Morrison, Julia E. and Smith, James A. (Dec. 2002). "Stochastic modeling of flood peaks using the generalized extreme value distribution". In: *Water Resources Research* 38.12, pp. 41–1–41–12. ISSN: 00431397. DOI: 10.1029/2001WR000502.

Papalexiou, Simon Michael and Koutsoyiannis, Demetris (Jan. 2013). "Battle of extreme value distributions: A global survey on extreme daily rainfall". In: *Water Resources Research* 49.1, pp. 187–201. ISSN: 00431397. DOI: 10.1029/2012WR012557.

Perica, Sanja, Martin, Deborah, Pavlovic, Sandra, Roy, Ishani, Laurent, Michael St., Trypaluk, Carl, Unruh, Dale, Yekta, Michael, and Bonnin, Geoffrey (2013). *Precipitation-Frequency Atlas of the United States Volume 9 Version 2.0: Southeastern States (Alabama, Arkansas, Florida, Georgia, Louisiana, Mississippi)*. Silver Spring, Maryland: U.S. Department of Commerce National Oceanic and Atmospheric Administration National Weather Service.

Prescott, P. and Walden, A. T. (1980). "Maximum likelihood estimation of the parameters of the generalized extreme-value distribution". In: *Biometrika* 67.3, pp. 723–724. ISSN: 0006-3444, 1464-3510. DOI: 10.1093/biomet/67.3.723.

Reed, D. W., Faulkner, D. S., and Stewart, E. J. (June 30, 1999). "The FORGEX method of rainfall growth estimation II: Description". In: *Hydrology and Earth System Sciences* 3.2, pp. 197–203. ISSN: 1607-7938. DOI: 10.5194/hess-3-197-1999.

Stewart, E. J., Jones, D. A., Svensson, C., Morris, D. G., Dempsey, P., Dent, D. E., Collier, C. G., and Anderson, C. W. (Mar. 2010). *Reservoir Safety – Long Return Period Rainfall*. R&D Technical Report WS 194/2/39/TR Volume 1 (Part 1). Joint Defra/Environment Agency Flood and Coastal Erosion Risk Management Research & Development Programme.

Von Mises, R. (1936). "La distribution de la plus grande de n valeurs". In: *Rev. Math. Union Interbalcanique* 1. Reprinted in Selected Papers II, pp. 271–294, Amer. Math. Soc., Providence, RI., 1954., pp. 141–160.

Weibull, Waloddi (1939). *A Statistical Theory of the Strength of Materials*. 151. General Staff Lithographic Institution (Generalstabens Litografiska Anstalts). Academy of Engineering Sciences (Ingeniörs Vetenskaps Akademiens), p. 45.

Woodward, Donald E. (May 2010). "Chapter 15 Time of Concentration". In: *NRCS Engineering Handbook (Part 630 Hydrology)*. United States Department of Agriculture Natural Resources Conservation Service, p. 29.